The metastable phase responsible for peak hardness in the ageing temperature range 403–483 K for an Al-Mg-Si ternary alloy

K. FUKUI, M. TAKEDA, T. ENDO
Department of Materials Engineering (SEISAN), Faculty of Engineering, Yokohama National University, 79-5 Tokiwadai, Hodogaya-ku, Yokohama 240-8501, Japan

A complicated precipitation behavior that is significantly dependent on aging temperature and chemical composition was reported in an aluminum-based Al-Mg-Si alloy. The precipitation behavior in the alloy has not been fully understood, despite the considerable literature [1–8] devoted to the subject. Systematic research into the aging process, taking into account the alloy composition, temperature, and time, is essential to elucidate the precipitation behaviors. However, very few works have examined the relationship between the macroscopic properties such as microhardness, the thermal stabilities of phases, and the microstructures. A recent study based on a combination of Vickers microhardness tests, differential scanning calorimetry (DSC) measurements, and transmission electron microscopy (TEM) examined the precipitation behavior appearing in the alloy [9–12]. The authors suggested that the formation of the metastable β" phase was detected around 510–600 K in the DSC measurement; and that this phase was mainly responsible for the hardness and small Si-rich particles with an ellipsoidal shape. However, a more quantitative relationship between peak hardness and the amount of β" precipitate was still undeveloped. This work was aimed to obtain the quantitative relationship between peak hardness and amount of β" precipitates, and also the relationship between time to peak hardness and time to maximum β" precipitate amount within the wide aging-temperature range 403–483 K.

Three Al-Mg-Si alloy specimens with balance compositions (Mg/Si = 2 in atomic ratio) were examined in this work. The chemical compositions of the alloy are listed in Table I. The 75 mm-diameter billets were extruded at 773 K and sheets formed by cold rolling. The final test specimens were solution treated at 828 K for 3.6 ks and subsequently quenched in ice water. Then they were isothermally aged in an oil-bath at 403 K, 433 K, 463 K, and 483 K. A Hitachi H-800 and Topcon EM-002B microscope were used at 175 and 180 kV accelerating voltage, respectively. Bright-field TEM and high-resolusion TEM (HRTEM) images were taken along the crystallographic ⟨001⟩ orientation in the Al matrices. The DSC measurements were carried out using a Rigaku TAS300-8230D instrument with a heating rate of 0.17 Ks^{-1}.

Fig. 1 shows the Vickers microhardness changes over aging time. The Hv curves obtained with a high (B1), an intermediate (B2) and a low (B3) solute concentration are shown in Fig. 1a–c, respectively. On annealing at 483 K, peak hardness values of 108, 78, and 42 Hv were obtained for B1, B2 and B3, respectively (Fig. 1a–c). Thus the peak hardness considerably decreases as the solute concentration decreases, and a similar tendency is observed at other aging temperatures. Fig. 1a–c show that the peak hardness increases and the time to the peak hardness increases at lower aging temperatures for the different solute compositions. We see that the peak positions of the Hv curves for the B1–B3 specimens aged at 403–463 K are linearly arranged in Fig. 1a–c and the slope of the straight line increases as the solute concentration decreases.

Fig. 2 shows bright-field TEM images of the microstructures of the B2 specimen after aging for peak hardness at 403–483 K. Needle-like and granular precipitates are common in each TEM image as reported in [12]. Microstructures obtained at lower temperatures show that the precipitates accompany high strain contrast and exhibit shorter needle-like precipitates. The specimens aged at 403 and 433 K show that the precipitates are more densely formed than specimens aged at 463 and 483 K. This supports that the specimens aged at lower temperatures have higher hardness. Fig. 3a shows the HRTEM image of a short needle-like precipitate in the B2 specimen aged at 403 K for 2400 ks. Fig. 3b shows the HRTEM image of a needle-like and two granular precipitates for the B2 specimen aged at 433 K for 600 ks. The lattice fringes of both needle-like precipitates shown in Fig. 3a and b are very similar to {200} of Al matrices. Fig. 3b shows two types of granular precipitate with regular and unclear fringes. A research paper describing the details of the HRTEM images is now in preparation for submission.

We applied the DSC measurement to the B2 specimens, which were as-quenched and aged at 403 K, 433 K, 463 K, and 483 K. Fig. 4 shows the DSC curves for the B2 specimens as-quenched and aged at 403 K. The DSC curve of the as-quenched specimen has four large exothermic peaks at approximately 350 K (peak K), 550 K (peak P), 580 K (peak Q), and 730 K (peak S), respectively. We attribute the first exothermic

TABLE I Composition (at.%) of the specimen studied

Alloy	Mg	Si	Al	Mg_2Si
B1	1.15	0.58	bal	1.59
B2	0.75	0.41	bal	1.12
B3	0.48	0.27	bal	0.73

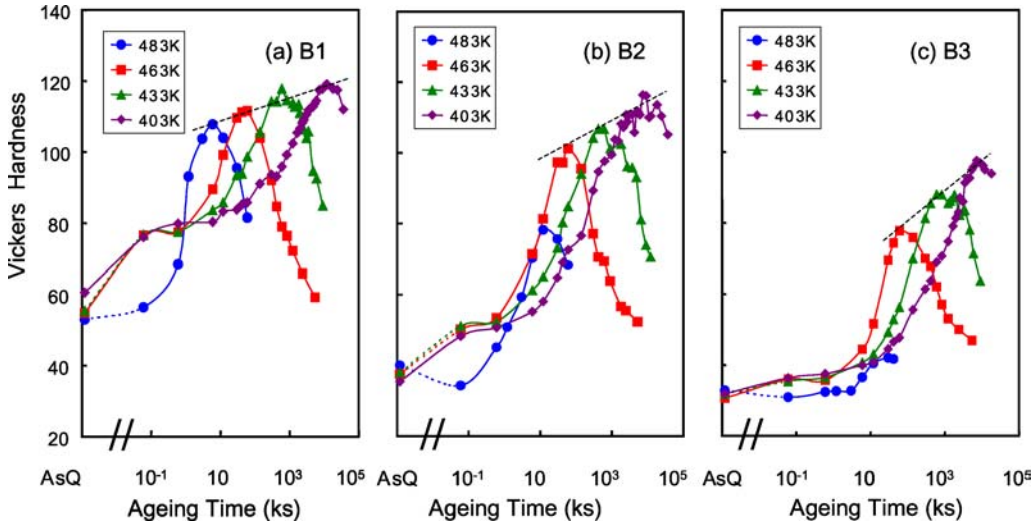

Figure 1 Vickers microhardness curves.

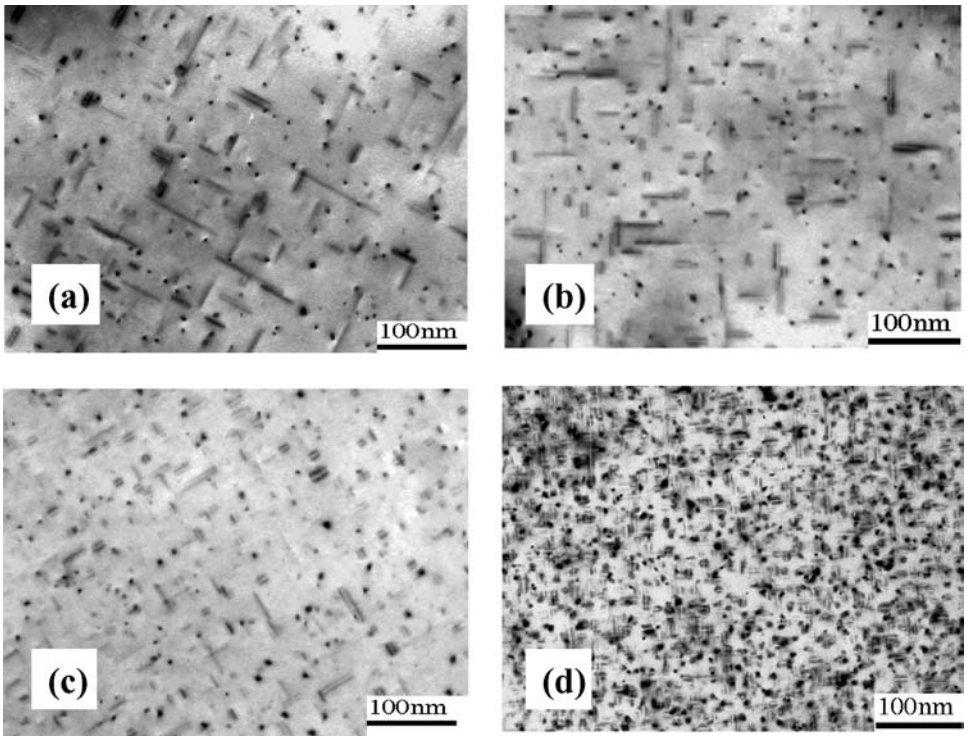

Figure 2 Bright-field TEM images of microstructures of B2 specimens isothermally aged (a) at 483 K for 12 ks, (b) at 463 K for 60 ks, (c) at 433 K for 420 ks, and (d) at 403 K for 7200 ks.

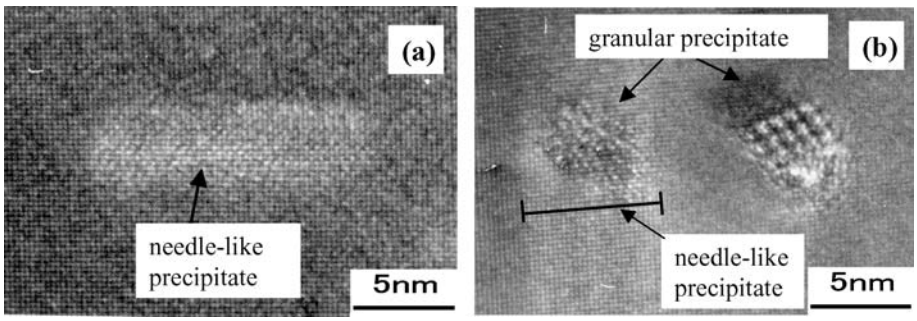

Figure 3 HRTEM images of the precipitates of B2 specimens aged (a) at 403 K for 2400 ks and (b) at 433 K for 600 ks.

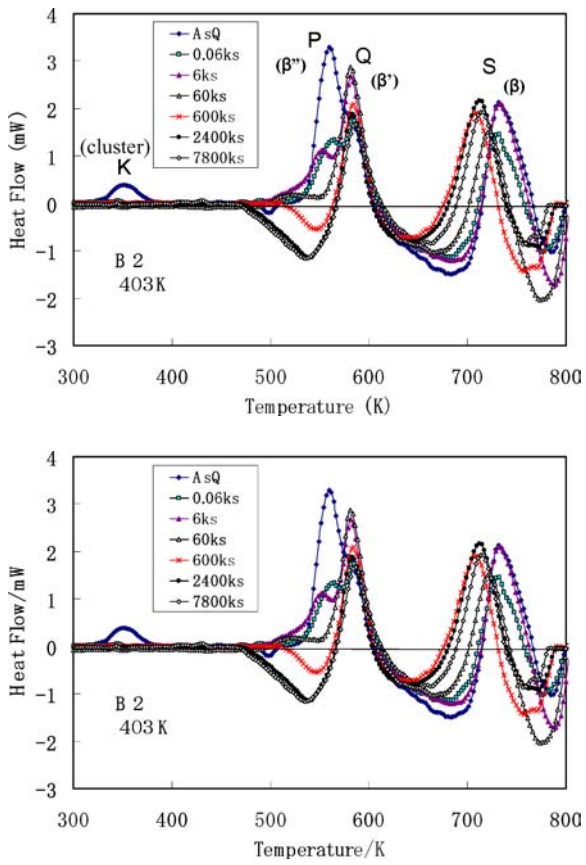

Figure 4 DSC curves for B2 specimens as-quenched and aged at 403 K.

peak K to solute clusters, the second peak P to the metastable β" phase, the third peak Q to the metastable β' phase, and the fourth peak S to the stable β phase on referring to [4]. While the second peak P is seen to consist of two separate exotherms b1 (GP-T zone) and b2 (the β" phase) in that paper [4], we apply the β"phase to the second peak P by the reasons that peak temperature of P is close to b2 peak and that b1 peak disappears with pre-aging. The exothermic peak is reduced by the isothermal annealing prior to the DSC measurement. This occurs because the supersaturation of the solute atoms is decreased by the pre-aging. Thus, reduction of the peak corresponds to the precipitation. We denoted the heat for peak P of the as-quenched and aged specimens as h_{AsQ} and h, respectively. Fig. 5a shows

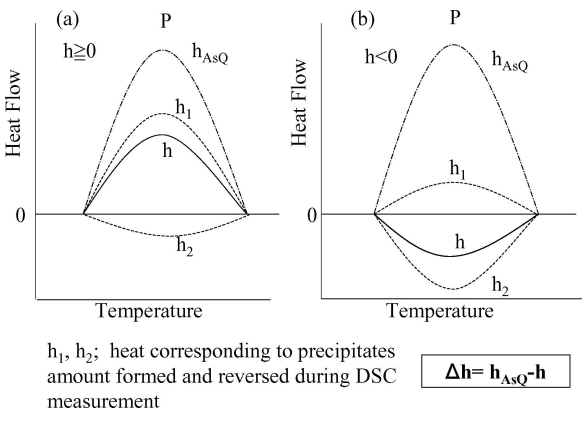

Figure 5 The heat corresponding to precipitates amount formed during isothermal annealing; Δh.

the quantity $\Delta h = h_{\mathrm{AsQ}} - h$ in case of peak P, which corresponds to the amount of β" precipitates in the case of $h \geqq 0$. The heat h appearing after isothermal annealing apparently shows the residue of the precipitation occurring during isothermal annealing. Heat h, however, resulted from the balance of the residual precipitation h_1 and the reversion h_2 in the DSC measurement. Following the above consideration, the negative balance possibly arose from the fact that the precipitation in the isothermal annealing was comparatively large and the reversion h_2 surpassed the residual heat h_1, as shown in Fig. 5b. The reduction of the peak P appeared more explicitly for the specimens isothermally aged at lower temperatures. Taking into account the fact that $\Delta h = h_{\mathrm{AsQ}} - h$ corresponds to the amount of β" precipitates, the β" phase was fully precipitated when Δh reached the maximum:$\Delta h_{\max} = h_{\mathrm{AsQ}} - h_{\min}$, where $h_{\min}$ corresponds to the heat at the minimum level. As the P and Q peaks were partly superimposed, we separated the two peaks and measured the area of each peak using computer software (GRAMS/32). We finally obtained the heat per unit mass by measuring the separated areas. Fig. 6 shows the changes in the Δh versus ageing time for the peak P of the B2 specimens aged at 403 K, 433 K, 463 K, and 483 K. The curves in Fig. 6 are similar to the hardness curves for the B2 in Fig. 1b.

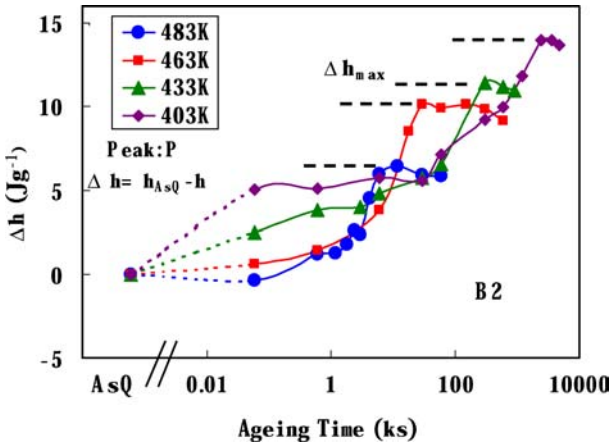

Figure 6 Relationship between Δh and ageing time for peak P.

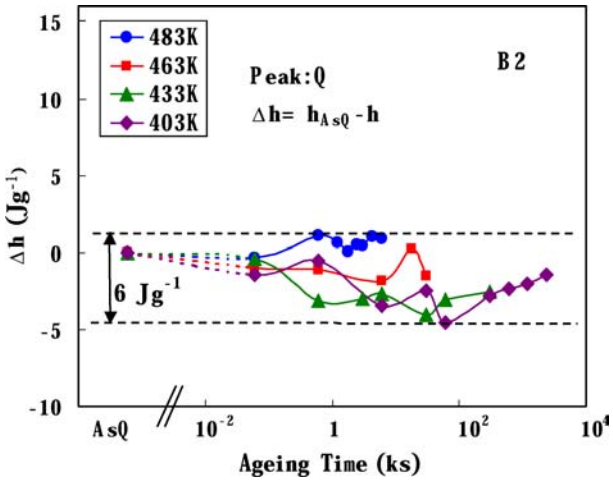

Figure 7 Relationship between Δh and ageing time for peak Q.

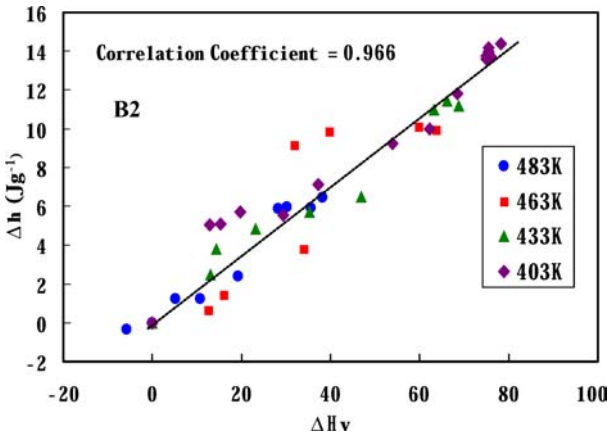

Figure 8 The correlation between Δh of peak P and ΔHv.

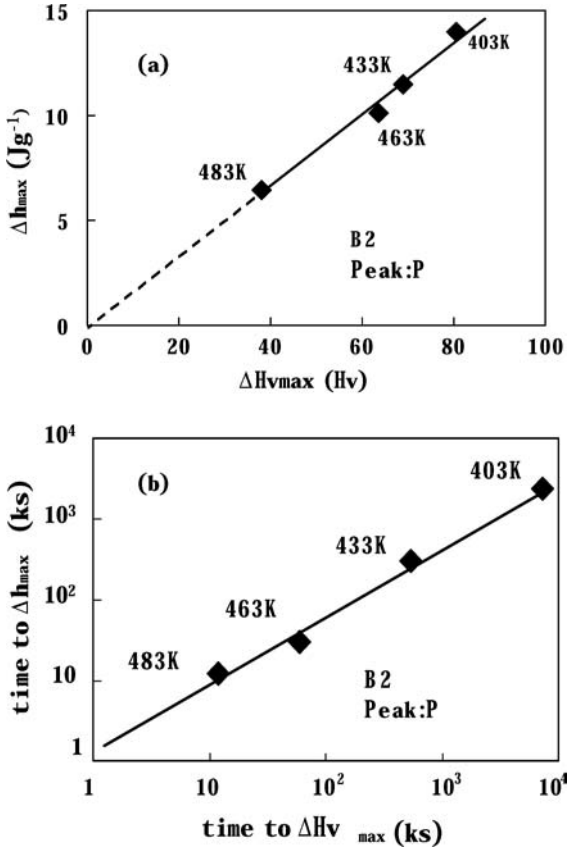

Figure 9 (a) Relationship between Δh_{max} of peak P and ΔHv_{max}, and (b) relationship between time to Δh_{max} of peak P and time to ΔHv_{max}.

The value of Δh_{max} and time to Δh_{max} both increase at lower temperatures. That is, the maximum density of the β" precipitates is considered to increase as the aging temperature decreases. Fig. 7 shows the changes of peak Q (Δh) with respect to aging time for the B2 specimens aged at 403 K, 433 K, 463 K, and 483 K. Little change in peak Q occurred at the aging temperature, and the range of theΔh was 6 Jg^{-1}, which was much less than for peak P. Therefore, we concluded that little precipitation of β' occurred.

To consider the precipitation-hardening in the Al-Mg-Si alloy, we examined the relationship between the heat Δh of peak P estimated by the present study and the Vickers microhardness. Fig. 8 shows the relationship between Δh and ΔHv at 403 K, 433 K, 463 K and 483 K. We defined ΔHv as the increment Hv from the as-quenched state. We obtained a very high correlation coefficient, 0.966. Fig. 9a shows the relationship between Δh_{max} and ΔHv_{max} at four different aging temperatures, where Δh_{max} and ΔHv_{max} are the maximum values of Δh and ΔH, respectively. Four markers are almost arranged in a straight line passing through the origin. It is revealed that the peak hardness is attained mainly by the metastable β" phase across the wide aging temperature range 403–483 K. Fig. 9b shows the relationship between the time to Δh_{max} and ΔHv_{max} for the B2 sample. The time relationship can also be expressed as a straight line. These facts lead to the conclusion that the maximum precipitate quantity of the metastable β" phase corresponds to the peak hardness.

In conclusion, the peak hardness is mainly attained by the metastable β" phase in the temperature range. The present work revealed the quantitative relationship between peak hardness and the β" precipitate amount in an Al-Mg-Si alloy, through a combination of DSC measurements, Vickers hardness tests, and TEM observations. The maximum peak reduction Δh_{max} of peak P in the DSC measurements was almost proportional to the maximum increase in hardness from the as-quenched state ΔHv_{max} in the aging temperature range 403–483 K.

References

1. G. THOMAS, *J. Inst. Metals.* **90** (1961–1962) 57.
2. M. H. JACOBS, *Philos. Mag.* **26** (1972) 1.
3. P. BARCZY and F. TRANTE, *Scand. J. Metals* **4** (1975) 284.
4. I. DUTTA and S. M. ALLEN, *J. Mater. Sci. Lett.* **10** (1991) 323.
5. G. HUPPERT, E. HORNBOGEN, *et al.,* in Proceedings of the 4th International Conference on Aluminum Alloys, edited by T. H. Saunders *et al.* (Atlanta, 1994) p. 628.
6. H. W. ZANDBERGEN, S. J. ANDERSEN and J. JANSEN, *Science* **277** (1997) 1221.
7. K. MATSUDA, T. SATO, S. IKENO, *et al., J. Jpn. Inst. Light Metals* **47** (1997) 493.
8. G. A. EDWARDS, K. STILLER, *et al., Acta Mater.* **46** (1998) 3893.
9. M. TAKEDA, F. OHKUBO, T. SHIRAI and K. FUKUI, in Proceedings of the 5th International Conference on Aluminium Alloys, edited by J. H. Driver *et al.* (Grenoble, 1996) p. 817.
10. M. TAKEDA, T. SHIRAI, S. SUHMEN, K. FUKUI and M. SAKAGUCHI, in Proceedings of the 6th International Conference on Aluminum Alloys, edited by T. Sato *et al.* (Toyohashi, 1998) p. 609.
11. M. TAKEDA, F. OHOKUBO, T. SHIRAI and K. FUKUI, *J. Mater. Sci.* **33** (1998) 2385.
12. M. TAKEDA, T. KURUMIZAWA, S. SUMEN, K. FUKUI and T. ENDO, *Z. Metallkd.* **93** (2002) 523.

Received 27 July
and accepted 19 October 2004